AIP | Review of Scientific Instruments

Velocity-map imaging at low extraction fields

Daniel A. Horke, Gareth M. Roberts, Julien Lecointre, and Jan R. R. Verlet

Citation: Review of Scientific Instruments **83**, 063101 (2012); doi: 10.1063/1.4724311
View online: http://dx.doi.org/10.1063/1.4724311
View Table of Contents: http://scitation.aip.org/content/aip/journal/rsi/83/6?ver=pdfcov
Published by the AIP Publishing

Velocity-map imaging at low extraction fields

Daniel A. Horke, Gareth M. Roberts, Julien Lecointre, and Jan R. R. Verlet[a)]
Department of Chemistry, University of Durham, South Road, DH1 3LE Durham, United Kingdom

(Received 30 March 2012; accepted 17 May 2012; published online 5 June 2012)

We present a velocity-map imaging (VMI) setup for photoelectron imaging that utilizes low electric extraction fields. This avoids any complications that could arise from electrostatic interactions between the extraction field and the molecular properties that are probed and has a minimal effect on the trajectory of ions in ion beam experiments. By using an attractive potential supplied to the detector, and keeping the electrodes at ground (zero) potential, we show that fringe fields between the VMI arrangement and the vacuum chamber can be eliminated, which is important in experiments on ions. © *2012 American Institute of Physics*. [http://dx.doi.org/10.1063/1.4724311]

I. INTRODUCTION

Charged-particle imaging techniques[1] and in particular velocity-map imaging (VMI) introduced by Eppink and Parker[2] have revolutionized photoelectron and photofragment spectroscopy and have become essential tools in molecular dynamics experiments.[3–7] In photoelectron spectroscopy, VMI has found applications for electrons with kinetic energies ranging from a few meV in slow-electron velocity-map imaging experiments[8] to tens of eV in experiments performed at synchrotrons or free-electron lasers.[9] The key attribute of charged-particle imaging is that it recovers not only the recoil speed information, but also directional information in the form of angular distributions. Under certain conditions, the raw images can be reconstructed to recover the full 3D Newton sphere of detected particles relative to the polarization of the light source ($\boldsymbol{\varepsilon}$). The original VMI spectrometer consists of a three- electrode arrangement, comprising a repeller, extractor, and ground electrode and this design is by far the most common arrangement.[2] The central orifices in the extractor and ground electrodes create an electrostatic lens that leads to the focusing of particles with the same velocity vector originating from any point in an interaction volume onto a specific point on a spatial plane. At this plane, a position sensitive detector (typically a pair of micro-channel plates (MCPs) coupled to a phosphor screen or delay line anode) detects the impact coordinates of the charged particles and, when collected over many impacts, generates velocity-map images. These measured 2D images can then be used to reconstruct the original 3D charged particle distribution, which ultimately provides access to the 1D speed distribution *via* angular integration.[7]

While most experimental VMI spectrometers are based on the original gridless three electrode design,[2] there have been a number of variations on this with additional electrodes introduced to improve the overall resolution of the spectrometer.[10,11] Alternatively, Papadakis and Kitsopoulos have shown that the arrangement can be simplified using only two specifically shaped electrodes to generate the desired electrostatic lens and a single field.[12] Although different geometries can meet the VMI condition, all the designs have in common the use of a large extraction field, with typical field strengths in the range of hundreds of V cm^{-1}. In many cases, these fields have a negligible effect on the spectroscopy or dynamics of the system in question. However, there are instances where this is not the case, such as high-lying Rydberg states which are very sensitive to electric fields due to the Stark shift.[13] An exception to such large extraction fields is the design introduced by the Liu group for time-sliced VMI of ions.[14] This design consists of 29 stacked electrodes creating two homogenous electric field regions. Ions up to 1.2 eV can be imaged on a 75 mm diameter detector following extraction from the interaction region in an electric field of ∼21 V cm^{-1} and acceleration in the second region with a field of ∼44 V cm^{-1}. While this design significantly reduces the extraction fields, it requires an elaborate setup of many electrodes and two separate electric field regions.

Here we present a new VMI arrangement that operates at electric fields far lower than the design presented by the Liu group,[14] requiring only ∼2.5 V cm^{-1} in the interaction region to image 1.2 eV photoelectrons on a 40 mm diameter detector. An important disadvantage of using small extraction fields is the low impact energy of the charged particles on the position sensitive detector. While this is less critical for the detection efficiency of electrons, it has a detrimental effect on heavier particles and we anticipate that imaging of ions will not be feasible in the current setup, and will probably require an additional acceleration field before the imaging detector to increase the impact energy.[7,15] Similar to the two-electrode design,[12] our spectrometer uses only a single potential to generate the electrostatic lensing fields. The presented design is motivated by the fact that we perform time-resolved photoelectron spectroscopy experiments on anions.[16,17] Using standard VMI spectrometers leads to a large deflection of the primary ion beam as it perpendicularly traverses through the spectrometer, which is undesirable if the ions after the VMI spectrometer are to be monitored or the photo-products analyzed using a secondary mass-spectrometer. Although the deflection problem can be alleviated by rapidly switching the VMI voltages on and off, the compact VMI spectrometer presented here circumvents this need and operates in a continuous mode.

a)j.r.r.verlet@durham.ac.uk.

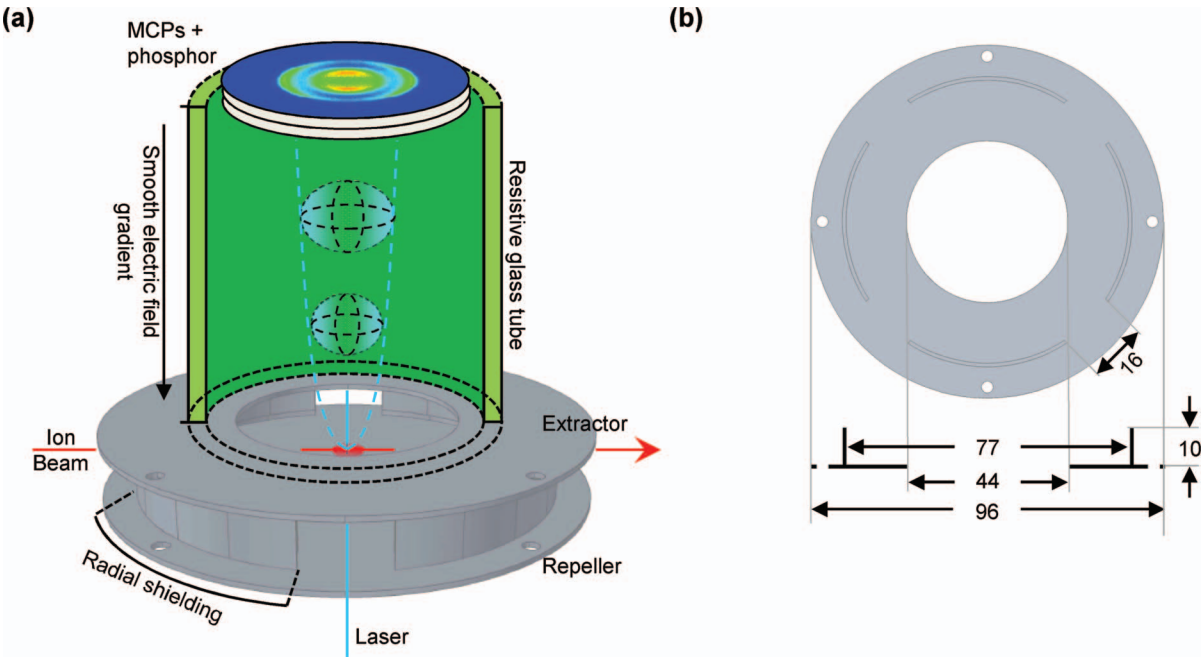

FIG. 1. (a) Schematic of the low-field velocity-map imaging setup. The two μ-metal electrodes and the resistive glass tube connected to the front of the position sensitive detector, create an electrostatic lens at the center of the electrodes and the glass tube creates a constant field gradient. Photoelectrons are guided by this field and VMI focused by the lens onto the detector. The low electric fields in the arrangement lead to minimal deflection of the ion beam. (b) Construction drawing of the VMI extractor plate manufactured from μ-metal, all dimensions are given in mm.

II. EXPERIMENTAL SETUP

A schematic of the VMI spectrometer is shown in Fig. 1(a). It consists of two 96 mm diameter and 1 mm thick electrodes manufactured from μ-metal (Magnetic Shields Ltd.). The lower (repeller) electrode is solid, while the upper (extractor) electrode (shown in Fig. 1(b)) has a central orifice of 44 mm to allow electrons to pass through and to create the VMI lens. The separation between the electrodes is 16 mm. Both electrodes have radial shielding to avoid the effects of any stray fields as shown in Fig. 1(b). The shielding is 10 mm in height on either plate and offset radially, such that when assembled it overlaps without being in contact (inner diameters are 81 mm and 77 mm for the repeller and extractor, respectively). The plates were manufactured by welding the shielding onto the flat electrode plate, with all welds achieved from the outside only, preserving a clean surface within the interaction region. The ion beam and detachment laser pass through square holes (16 mm $\times$ 16 mm) in this shielding, which are situated perpendicular to each other. A 49.9 mm long resistive glass tube (inner diameter 48.3 mm, outer diameter 63.5 mm; Photonis Inc.) is sandwiched between the extractor and the front of a position sensitive detector and is held in place by a 1 mm thick Teflon ring. Both ends of the resistive glass tube are metalized (nickel coating) to ensure electrical contact with the extractor on one end and the front plate of the detector on the other. By applying a potential difference across the glass tube, a constant electric field gradient is created inside the tube and accelerates electrons towards the detector. The front plate of the detector consists of a 2 mm thick stainless steel ring with a 44 mm orifice that exposes a 40 mm diameter active area MCP pair. The total distance between the laser-ion interaction point and the detector is 60 mm. The outside of the glass tube is surrounded by a μ-metal cylinder to further eliminate stray magnetic fields.

The potential difference between the extractor electrode and the front of the detector forms a linear electric field gradient. The electrostatic lens leading to the VMI condition is formed by the inhomogeneous field that leaks from the central orifice in the extractor electrode (shown in Fig. 2(a)). Although the two electrodes can be held at different potentials, the current VMI spectrometer has been designed such

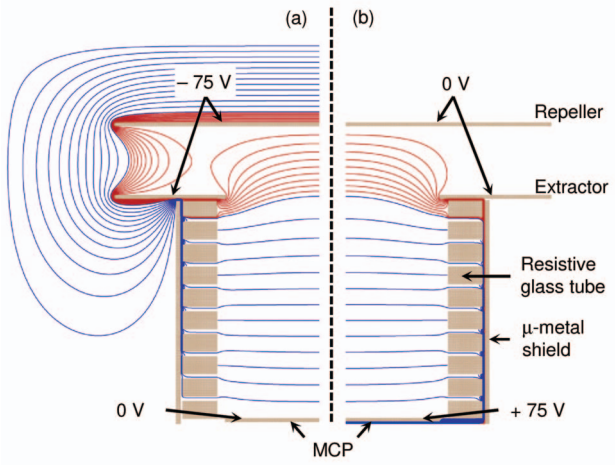

FIG. 2. SimIon 8.0 simulation of the contour lines present in our VMI setup. A central slice through the detector is shown for (a) traditional imaging with a potential (−75 V) applied to the electrodes and the detector front at 0 V and (b) imaging in which the electrodes are at 0 V while the front of the detector is held at a potential (+75 V). Red field lines are spaced by 1 V, blue field lines are spaced by 5 V. In (b), the fringe fields present at the edges of the electrodes seen in (a) are completely avoided.

that there is no potential difference between the two electrodes and both electrodes are connected to the same power supply. This condition can be achieved by varying the ratio of the orifice diameter in the extractor to the electrode separation. In the present design, this ratio is 44.0 mm:16.0 mm = 2.75, which leads to the VMI focal plane being located 60 mm from the center of the detector for a ratio of electrode potentials $V_{\text{extractor}}$:$V_{\text{repeller}} = 1$. Changing the ratio of electrode dimensions leads to a change in the location of the VMI focal plane. An interesting feature of this is that when the electrode dimensions ratio >2.75, the ratio $V_{\text{extractor}}$:V_{repeller} >1, which implies that a higher potential is required on the extractor than the repeller.

The incorporation of the resistive glass tube between the extractor electrode and the front of the detector enables the construction of a very compact VMI spectrometer. The smooth field gradient inside the glass tube serves to avoid the usual diverging lens in the traditional VMI design.[2] Specifically, in a traditional VMI arrangement, the electrostatic lens decreases the angular divergence of the charged-particle cloud between the repeller and extractor, but increases it between the extractor and the third ground electrode. In the current design, this divergent lens between extractor and the ground electrode is eliminated which reduces the curvature of the focal plane (achromatic aberrations), allowing for the short flight path. In our design, the 2 mm retaining ring for the MCPs of the detector leads to a small field distortion just before the MCPs, which has a similar effect as the diverging lens in the traditional VMI design, albeit much weaker. This could, in principle, be avoided by using a thinner retaining ring.

The position sensitive detector consists of two 40 mm active area MCPs in a chevron geometry, coupled to a phosphor screen (Photek Ltd., VID240). The front face of the detector can be held at a variable potential. The resulting image is captured with a CCD camera (Basler A312f, 512 × 512 pixels) and subsequently deconvoluted with the polar onion-peeling algorithm to yield photoelectron kinetic energies and angular distributions.[18] The overall dimensions are such that the entire VMI spectrometer, which is mounted on the DN100CF flange of the position sensitive detector, is confined to a 6 in. cube with the interaction point at its center.

As the repeller and extractor electrodes are at the same potential, the electrostatic lens leading to the VMI condition is formed solely by the electric field leaking from the central orifice in the extractor electrode. This leads to a very low electric extraction field in the interaction region and furthermore eliminates problems arising from fluctuating power supplies as both plates are controlled by a single supply. For photoelectron imaging, the extraction field can be created by applying a negative voltage to the electrodes and grounding the front face of the detector. The contour lines of the electric fields for this VMI arrangement are shown in Fig. 2(a) for a voltage of −75 V supplied to the electrodes (which can image electrons up to ∼2 eV onto a 40 mm active detector area). Contour lines are simulated using SimIon 8.0 (Scientific Instrument Services Inc., USA). For the simulations the radial shielding is not included, and we note that inclusion of the gaps in the shielding does not affect the electrostatic lens at −75 V. The resistive glass tube is approximated by a stack

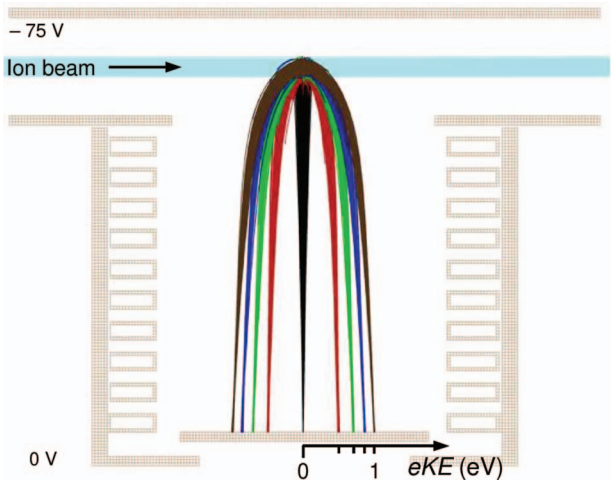

FIG. 3. SimIon 8.0 simulation of electron trajectories corresponding to kinetic energies of 0.0, 0.25, 0.5, 0.75, and 1.0 eV, imaged with a VMI voltage of −75 V.

of 10 ring electrodes producing a linear electric field gradient between the extractor and the detector plate. The contours shown in Fig. 2(a) clearly show the electrostatic lens formed in the interaction region. Aberrations at the edge of the resistive tube are an artifact of the simulation and arise from the use of 10 electrodes instead of the infinite series of electrodes that constitutes the glass tube.

Figure 3 shows a central slice through a simulation of electron trajectories for isotropic electrons distributions with 0.0, 0.25, 0.75, and 1.0 eV of kinetic energy and the VMI potential set at −75 V. The electrons are simulated starting from a normal distribution around the center of the imaging spectrometer (standard deviation of 0.5 mm) to account for the finite diameter of ion and laser beams. Also shown is the simulated path of a primary ion beam (kinetic energy 2.3 keV and $m/z = -127$ Da, corresponding to the experimental conditions of an I^- ion beam), highlighting the almost negligible beam deflection as it traverses through the VMI spectrometer. Cleary observed is the focusing effect of the electrons on the focal plane at the MCP detector. We calculate a magnification factor of $M = 1.3$ for our setup. The photoelectron cloud initially expands in the low-field interaction region, while being extracted and subsequently focused on the detector. The low electric fields and initial expansion of the electron cloud result in a relatively long (30 ns) flight time.

The current VMI spectrometer has been primarily designed with the aim of reducing the deflection experienced by an ion beam traversing a standard VMI arrangement. Hence, a small extraction field is desirable. Although the local field strength at the interaction point is small, there is a significant field where the ion beam enters and exits the spectrometer. These fringe fields arise from the potential difference between the electrodes and the surrounding vacuum chamber. As these fringe fields are inhomogeneous, they will lead to a lensing effect on any ion beam propagating through the arrangement. Fringe fields can be completely avoided by keeping the VMI electrodes grounded and applying an attractive potential to the front of the detector to generate the lens and guide the electrons. The resultant field lines in such an arrangement are

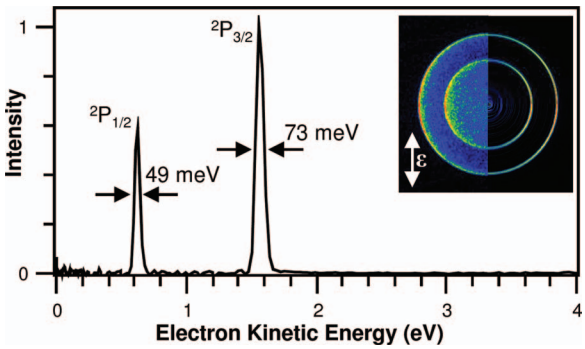

FIG. 4. Photoelectron spectrum for the photodetachment from iodide at 4.63 eV (268 nm) with a femtosecond laser. Shown inset is the raw (left half) and deconvoluted reconstructed (right half) photoelectron image. The laser polarization is indicated by $\boldsymbol{\varepsilon}$.

shown in Fig. 2(b), where both electrodes are at ground potential and the front of the detector is held at +75 V.

A full description of our anion photoelectron imaging spectrometer has been given previously.[19,20] For the photoelectron images presented here, two detachment laser systems are used. Light at 355 nm is generated by third harmonic generation of the output of a commercial Nd:YAG laser which is tuned to deliver ~5 mJ in a 10 ns pulse, operating at a 10 Hz repetition rate. UV photons at 268 nm are produced from third harmonic generation of the fundamental output from a commercial Ti:Sapphire femtosecond amplified system. This produces ~100 fs pulses and energies of ~20 μJ per pulse and data were collected at 200 Hz repetition rate.

III. RESULTS

We demonstrate the resolution at low extraction fields by imaging the photodetachment of electrons from iodide (I^-) at 268 nm (4.626 eV). The electron affinity of iodine is 3.059 eV,[21] leading to electron kinetic energies (*eKE*s) of 1.567 eV and 0.624 eV for electron detachment from I^- to the $^2P_{3/2}$ and $^2P_{1/2}$ spin orbit split states of neutral iodine, respectively. This was imaged at an electrode voltage of −300 V, leading to an electric field experienced by the ions in the interaction region of ~15 V cm^{-1}. The resulting photoelectron spectrum is shown in Fig. 4, along with the raw (inset, left) and central slice through the deconvoluted photoelectron image (inset, right). For the low *eKE* peak ($^2P_{1/2}$), we achieve a nominal resolution of $\Delta eKE/eKE$ ~8%. However, this is limited by the large bandwidth of the femtosecond laser system used and does not reflect the achievable resolution of our imaging detector. The $^2P_{3/2}$ feature ($eKE = 1.567$ eV) is recorded with a resolution of ~5%, the maximum resolution achievable with the current imaging setup.

Lower extraction fields can be employed to image slower electrons and we demonstrate this by imaging the photodetachment from I^- at 355 nm (3.493 eV), using electrode voltages of −75 V and a grounded detector front plate. In this case the electric field strength at the interaction point is less than 4 V cm^{-1}. The resulting photoelectron image and spectrum are shown in Fig. 5(a).

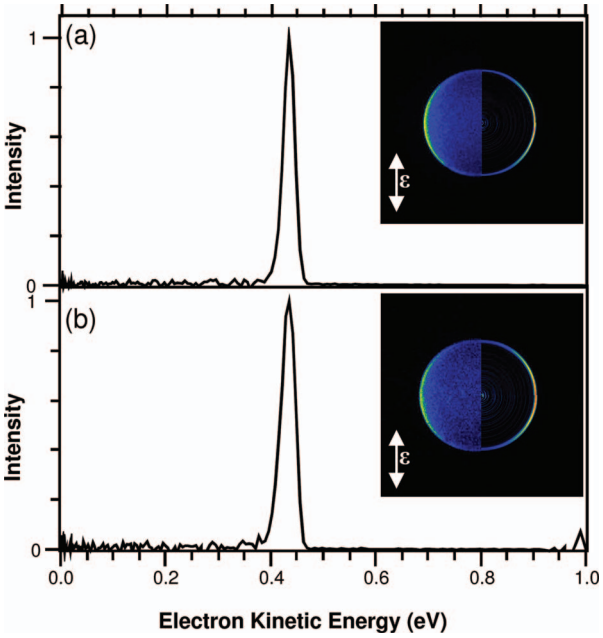

FIG. 5. Photoelectron spectra of iodide at 3.496 eV (355 nm) using (a) the traditional imaging in which the electrodes are held at a potential (−75 V) and (b) imaging in which the electrodes are held at near-ground potential (<−2 V) and the detector front plate at a positive potential (+75 V). Shown inset are the raw (left half) and deconvoluted reconstructed (right half) photoelectron images. The laser polarization is indicated by $\boldsymbol{\varepsilon}$.

Photoelectron imaging was also performed by grounding the electrodes while retaining the front of the detector at +75 V. This resulted in a very large amount of noise arising from background and could not be discriminated by a fast voltage gate on the MCPs. The stray electrons probably arise from the formation of electrons at surfaces that are struck by the laser outside of the VMI arrangement. These can then propagate into the spectrometer and are drawn up into the time-of-flight section (glass tube) and recorded on the detector. These stray electrons could be effectively removed by applying a very small (<−2 V) potential to the electrodes, which prevents background electrons produced by light scattering and ion gauges from entering the VMI spectrometer. The resultant image and spectrum is shown in Fig. 5(b). The performance of the spectrometer in this mode is comparable to that achieved with conventional imaging (e.g., Fig. 2(a)), as shown in Fig. 5(a).

We finally demonstrate the ability of using extremely low extraction fields and potentials for the collection of VMI images by using a 9 V battery as the power supply for the electrodes and retaining the front of the detector at ground. In this case, the electric field strength at the interaction point is <0.5 V cm^{-1}. This very low field imaging is demonstrated by imaging the photodetachment from bromide (Br^-) at 355 nm (3.496 eV). The electron affinity of bromine is 3.364 eV,[22] corresponding to an $eKE = 0.132$ eV for detachment at 355 nm. Figure 6 shows the photoelectron spectrum of Br^- which has been obtained from the raw image shown in the inset. The overall photoelectron signal is significantly lower because of the low impact energy of the electrons on the MCP, reducing the detection efficiency. The photoelectron peak has a full width at half maximum of 10 meV, corresponding to a

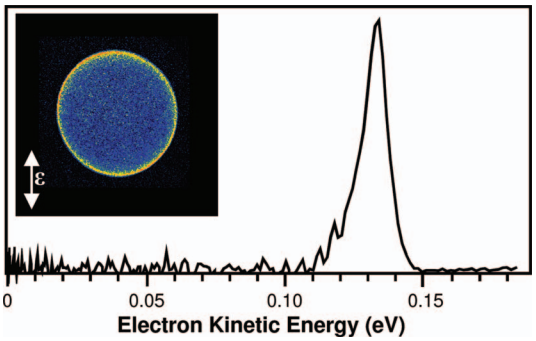

FIG. 6. Photoelectron spectrum for the photodetachment from bromide at 3.496 eV (355 nm). Inset is the raw photoelectron image. The extraction field was created solely by the potential supplied from a 9 V battery connected to the electrodes, while the front of the detector was held at 0 V. The laser polarization is indicated by $\boldsymbol{\varepsilon}$.

resolution $\Delta eKE/eKE$ <8%, which is approaching the resolution when the spectrometer is operated at higher electrode potentials. The image shows some distortions, as shown inset in Fig. 6. Specifically, the most prominent distortion is the moderate stretching of the image nominally along the vertical axis (by ~3%) and a modest tilting of the image relative to the laser polarization. In principle, one could manipulate the image to remove this distortion to produce a circular image, which would yield the expected resolution gained by imaging at higher potentials.

IV. DISCUSSION

The results presented demonstrate a simple VMI spectrometer consisting of only 2 electrodes and a resistive glass tube to produce a smooth electric field gradient. This enables photoelectron imaging with extremely low extraction fields, attaining resolutions typical for femtosecond photoelectron imaging spectrometers.[17,23] In the examples presented in Fig. 5, for both imaging voltage arrangements, the fields in the interaction region are on the order of 4 V cm^{-1}, while still yielding a respectable resolution for an imaging detection setup.

Employing low voltages yields several practical advantages. First, as only a single power supply is used, the long-term stability of the setup is increased and one is not prone to ripple voltage differences between the electrodes. Second, low voltages are considerably easier (and cheaper) to switch in short times, as is commonly done in coincidence imaging experiments.[24] Third, it will, in principle, allow photoelectron imaging of a continuous ion beam with a cw (or quasi-cw) light source, in which case pulsing would reduce the duty cycle. Finally, the VMI arrangement presented here was designed with the prevention of ion deflection in mind. To this end, for electrode voltages at −75 V, the setup presented deflects a 2 keV beam of iodide ions less than 0.1°. This allows the simultaneous monitoring of parent ions and photoelectrons for on-the-fly normalization of the photoelectron signal to the ion current. Moreover, it enables us to perform reflectron time-of-flight mass spectrometry on the ion packet or ionic products in parallel to photoelectron spectroscopy. For such experiments, it is critical that the fringe lensing fields on the entrance and exit of the VMI spectrometer are minimized and this is achieved by applying a positive potential to the top of the glass tube, and (near) grounding both VMI electrodes.

Using a 9 V battery as the power supply for imaging, as shown in Fig. 6, noticeably reduces the resolution which arises from distortions in the circularity of the image. These distortions are due to the greater sensitivity to any residual stray fields. Specifically, the presence of electric fields from nearby high-voltage sources can leak into the VMI arrangement. Such leakage fields have a negligible effect at higher operating potentials (i.e., <−50 V), but at −9 V the magnitude of the leakage fields becomes important relative to the low field strength of <0.5 V cm^{-1} at the interaction point. Additionally, the long flight time to the detector, which we determined to be ~87 ns based on simulations, will lead to a long interaction time for the electrons with stray fields. In our experiment, immediately following the VMI spectrometer, a deflector plate directs the ion packet onto a MCP that lies parallel to the VMI electrodes. Beyond this, a reflectron mass-spectrometer can return the ion packet and the same MCP detector can be used to monitor fragments by pulsing the deflector. Applying a normal operating potential of −1 kV to this deflector leads to a significant distortion of the image and reducing the spectral resolution to 14%. For the image shown in Fig. 6, both the deflector and MCP detector for the ions have been turned off. Despite this, there is clearly an additional source of interference and improvements could be made to ensure that the leakage fields are eliminated. Specifically, the electrodes could be redesigned to be made as a single piece and the apertures in the radial shielding covered by high-transmission mesh.

We point out that our spectrometer was designed for low extraction fields, rather than high resolution because, in general, the bandwidth of the femtosecond pulses used in our experiments is the limiting factor to determining our energy resolution, rather than the spectrometer. However, improvements in resolution can be made with tighter tolerances to the overall construction and additional lens elements can also be introduced to improve resolution at the expense of more complex arrangements. The use of a resistive glass tube to create a region of constant electric field gradient allows the construction of VMI setups with short flight paths, but extremely large dynamic ranges. Using electrode voltages of 1 kV allows imaging of electrons with up to 15 eV of kinetic energy. Indeed as the electrodes are in electrical contact, the extraction voltage is only limited by the breakdown voltage across the resistive coating of the glass tube, which is several tens of kV. Therefore, imaging of electrons with hundreds of eV kinetic energy is feasible.

V. CONCLUSION

We have demonstrated a velocity-map imaging setup designed for photoelectron imaging that uses only a single voltage supply and can be operated with typical extraction fields of <5 V cm^{-1}. The use of a resistive glass tube creates a smooth electric field gradient inside, "pushing" photoelectrons onto the position sensitive detector. By applying a potential to the detector, and grounding the VMI electrodes,

photoelectrons are "pulled" towards the detector, significantly reducing fringe fields protruding from the spectrometer. The use of low voltages and extraction fields minimizes the electric fields in the interaction region which: (i) can influence atomic or molecular properties; (ii) does not significantly affect ion beams that can subsequently be detected; and (iii) yields several practical and economic advantages. The use of resistive glass tubes allows the construction of short flight path VMI spectrometers with dynamic ranges spanning several orders of magnitude.

ACKNOWLEDGMENTS

This work has been supported by the EPSRC (EP/D073472/1) and Durham University. We are grateful to J. L. Nixon for his early contributions to the development of the spectrometer. We thank the EPSRC laser loan pool for loan of the ns laser system.

[1]D. W. Chandler and P. L. Houston, J. Chem. Phys. **87**, 1445 (1987).
[2]A. T. J. B. Eppink and D. H. Parker, Rev. Sci. Instrum. **68**, 3477 (1997).
[3]A. I. Chichinin, K. H. Gericke, S. Kauczok, and C. Maul, Int. Rev. Phys. Chem. **28**, 607 (2009).
[4]D. Townsend, M. P. Minitti, and A. G. Suits, Rev. Sci. Instrum. **74**, 2530 (2003).
[5]A. G. Suits and J. W. Hepburn, Annu. Rev. Phys. Chem. **57**, 431 (2006).
[6]R. Mabbs, E. R. Grumbling, K. Pichugin, and A. Sanov, Chem. Soc. Rev. **38**, 2169 (2009).
[7]B. J. Whitaker, *Imaging in Molecular Dynamics* (Cambridge University Press, Cambridge, England, 2003).
[8]D. M. Neumark, J. Phys. Chem. A **112**, 13287 (2008).
[9]G. A. Garcia, L. Nahon, C. J. Harding, E. A. Mikajlo, and I. Powis, Rev. Sci. Instrum. **76**, 053302 (2005).
[10]H. L. Offerhaus, C. Nicole, F. Lepine, C. Bordas, F. Rosca-Pruna, and M. J. J. Vrakking, Rev. Sci. Instrum. **72**, 3245 (2001).
[11]E. Wrede, S. Laubach, S. Schulenburg, A. Brown, E. R. Wouters, A. J. Orr-Ewing, and M. N. R. Ashfold, J. Chem. Phys. **114**, 2629 (2001).
[12]V. Papadakis and T. N. Kitsopoulos, Rev. Sci. Instrum. **77**, 083101 (2006).
[13]T. F. Gallagher, *Rydberg Atoms* (Cambridge University Press, 2005).
[14]J. J. Lin, J. Zhou, W. Shiu, and K. Liu, Rev. Sci. Instrum. **74**, 2495 (2003).
[15]J. Oberheide *et al.*, Meas. Sci. Technol. **8**, 351 (1997).
[16]A. Sanov and R. Mabbs, Int. Rev. Phys. Chem. **27**, 53 (2008).
[17]J. R. R. Verlet, Chem. Soc. Rev. **37**, 505 (2008).
[18]G. M. Roberts, J. L. Nixon, J. Lecointre, E. Wrede, and J. R. R. Verlet, Rev. Sci. Instrum. **80**, 053104 (2009).
[19]J. Lecointre, G. M. Roberts, D. A. Horke, and J. R. R. Verlet, J. Phys. Chem. A **114**, 11216 (2010).
[20]D. A. Horke and J. R. R. Verlet, Phys. Chem. Chem. Phys. **13**, 19546 (2011).
[21]R. J. Peláez, C. Blondel, C. Delsart and C. Drag, J. Phys. B **42**, 125001 (2009).
[22]C. Blondel, P. Cacciani, C. Delsart, and R. Trainham, Phys. Rev. A **40**, 3698 (1989).
[23]T. Suzuki, Annu. Rev. Phys. Chem. **57**, 555 (2006).
[24]C. Y. Ng, Int. J. Mass Spectrom. **200**, 357 (2000).